

## Structural and vibrational properties of a realistic model of amorphous silicon

K. Winer

*Max-Planck-Institut für Festkörperforschung, Heisenbergstrasse 1, D-7000 Stuttgart 80, Federal Republic of Germany*

(Received 14 July 1986; revised manuscript received 17 October 1986)

Calculations of the structural and vibrational properties of a 216-atom continuous-distorted-network model of amorphous silicon with periodic boundary conditions are presented and discussed. The pair correlation function and geometric distortions of the model are in good agreement with experiment. The eigenmodes of vibration are calculated using both the Keating and Weber interactions. The resulting phonon density of states and Raman and ir spectra also show good agreement with experiment. The results demonstrate that the model is representative of the bulk, homogeneous structure of amorphous silicon.

### I. INTRODUCTION

Amorphous silicon and its alloys have immediate and important applications in the fields of electronics and energy conversion technologies. Also, its simple chemical bonding and composition make amorphous silicon an ideal prototype for the study of the disordered solid state. Although the majority of effort has been concentrated on investigating its technologically useful properties, the central problem of amorphous silicon remains the determination of its structure at the atomic level.

Progress in this direction has been slowed by two factors. First, unlike the crystalline phases, there is no experimental technique available that can determine the coordinates of atoms in amorphous silicon. The most detailed experimental measure of its structure is a one-dimensional correlation function derived from x-ray or neutron diffraction data.<sup>1</sup> The very nature of this function precludes the unambiguous determination of the structure of amorphous silicon because, in principle, an infinite number of possible structures can be found that are consistent with the data. Most attempts to interpret the main features in the correlation function of amorphous silicon have relied on structural models, both hand-built and computer-generated.

The experimental correlation function provides a means of distinguishing between different types of competing structural models. The basic requirement of agreement with diffraction data has eliminated microcrystalline models, models based on polymorphic structures, and polytopic models from serious consideration as representatives of the bulk, homogeneous structure of amorphous silicon. It is now generally agreed that this structure is best represented by continuous-random-network models.<sup>1</sup> Because the correlation functions of completely random networks are in poor agreement with experiment,<sup>2</sup> I refer to the latter type of structural model as a continuous distorted network (CDN). In lieu of more direct experimental techniques, the most effective method of determining the structure of amorphous silicon seems to be through the study of CDN structural models.

Despite the relative maturity of this approach, standard model building techniques that lead to realistic amor-

phous silicon structures are not well developed. Since Polk constructed the first CDN model of amorphous silicon in 1971,<sup>3</sup> many of these models have been produced with structures in varying degrees of agreement with experiment. Each model can be distinguished by the number of atoms it contains, its method of construction, its boundary conditions, and by its geometric and topological distortions relative to the diamond structure. Attempts to draw general conclusions from a comparison of these models concerning the relative importance of specific structural properties are complicated by the significant variation of more than one characteristic parameter from model to model. The second major stumbling block to progress in determining the structure of amorphous silicon, therefore, has been the lack of a practical, systematic method of producing "standard" CDN structural models.

I propose three minimum criteria that such models should meet. First, the models should be computer-generated to eliminate the bias that can occur in hand-built models. Second, the models should have periodic boundaries, which are the most convenient and realistic way to terminate free surfaces. I make use of a further benefit of periodic boundaries in this study by allowing the inclusion of long-range forces in a straightforward manner. Of course, there is some question as to whether periodic boundary conditions are justified in amorphous silicon models when the implied long-range order is explicitly lacking in the real material. However, as long as the lattice constant of the unit cell is greater than the range of atomic correlations ( $\sim 10$  Å), the structure of a model can be a good approximation to that of real amorphous silicon. Finally, the correlation functions of the models should show no serious discrepancy with that of experiment. This last criterion is the most important. Models that do not meet this criterion simply must be rejected as representatives of amorphous silicon.

There have been several attempts<sup>2,4-6</sup> at using these criteria to produce realistic amorphous silicon structures, but only very recently have such attempts been successful. Wooten, Winer, and Weaire<sup>7</sup> (WWW) have developed a simple and practical algorithm for the systematic construction of large, periodic CDN models of amorphous silicon whose correlation functions show no serious

discrepancy with experiment. The fulfillment of the minimum criteria for "standard" model construction, however, does not guarantee that the resulting structures are also consistent with other available experimental measurements. The vibrational properties are particularly useful as a further test of the validity of structural models of amorphous silicon. These properties depend strongly on the local arrangement of atoms in the structure and therefore can serve as a sensitive guide for further model discrimination.

In the next section, I examine the structural properties of the most realistic CDN model yet produced by the WWW algorithm. In Sec. III, I examine the vibrational properties of the model including the Raman and infrared activities. On the basis of the calculated structural and vibrational properties of the model, I argue that it is a fairly realistic representation of the bulk, homogeneous structure of amorphous silicon and is therefore a worthy candidate for further investigation.

## II. STRUCTURAL PROPERTIES OF A CDN MODEL OF AMORPHOUS SILICON

The model I consider contains 216 atoms, has cubic periodic boundary conditions with a lattice constant of 16.2813 Å, is fully fourfold coordinated with no dangling bonds, and has been relaxed to an energy minimum with both Keating<sup>8</sup> and Weber<sup>9-11</sup> interactions. Standard measures of the geometric distortion for the model are compared with experiment in Table I.

The density at which the distortion energy is minimized for the model is slightly greater than that of the diamond structure. Diffraction experiments suggest that the density of amorphous silicon is slightly lower.<sup>1</sup> Other experiments yield densities either slightly above or below the crystalline density.<sup>12</sup> Because real amorphous silicon thin films contain voids and other defects, density comparisons with fully fourfold coordinated models, as well as many other quantitative comparisons, must not be given undue weight.

The essential difference between relaxing structures with the Keating potential and the Weber interactions is the effect of long-range (Coulomb) forces. The main effect observed in the CDN model is the significant reduc-

tion in the rms bond-length deviation without a corresponding large increase in the rms bond-angle deviation. This comes about because of the additional degree of freedom in the Weber interactions introduced by the off-axis positions of the bond charges.

Curiously, the distortion energy of the model is much higher when relaxed with the Keating potential. Although the Keating and Weber interactions are quite different, one can compare the dominant, short-range part of the Weber interactions with the Keating potential by defining an effective  $\beta/\alpha$ .<sup>9</sup> This turns out to be about 0.3, very close to the value used in the Keating potential. The vibrational properties of distorted structures calculated with the Weber interactions depend strongly on the bond-length distortions.<sup>11</sup> It is possible that, for the same angular distortion, the Weber distortion energy of some structure would be reduced from the Keating value by a lowering of the average bond strain. A more detailed understanding of the difference in distortion energies must await further investigation.

Comparisons of the bond-angle and bond-length distortions with those inferred from experimental correlation function or Raman peak widths must also be made with caution. Again, the presence of defects and impurities in real amorphous silicon films may complicate interpretations of distortion. The wide range of experimentally measured bond-angle deviations makes this clear.<sup>13</sup> The important point is that the model contains distortions near to those found in amorphous silicon.

A far more significant test of the model is to compare its pair correlation function with experiment as shown in Fig. 1. There is substantial agreement up to about 8 Å, which encompasses the first four peaks. The peaks beyond about 8 Å in the correlation function of the model are due to interference effects that occur at distances larger than half the lattice spacing. Although the agreement is far from perfect, and perhaps not within experimental error, it is sufficiently good to consider this model to be a representative "standard" model according to the criteria described in Sec. I.

The ring statistics for the model are shown in Table II. The immediately discernable difference between the model and the diamond structure is that the former has five- and seven-membered rings. In fact, every atom in the model

TABLE I. Structural characteristics of the CDN model.

	$\rho/\rho_0$	$\Delta r_{\text{rms}}$	$\Delta\theta_{\text{rms}}$	$\Delta E$ (eV/atom)
F-2 Si	1.00	0.0%	0.0%	0.00
Keating ( $\beta/\alpha=0.285$ )	1.04	2.6%	11.3°	0.32
Weber ( $\beta/\alpha=0.300$ )	1.03	2.2%	11.3°	0.20
Experiment	0.90 <sup>a</sup>	1.6% <sup>b</sup>	9.7° <sup>a</sup>	0.25 <sup>c</sup>

<sup>a</sup>Etherington *et al.* (Ref. 1).

<sup>b</sup>Temkin *et al.* (Ref. 13).

<sup>c</sup>Derived from the Keating potential by considering an rms angular distortion of 9.7°.

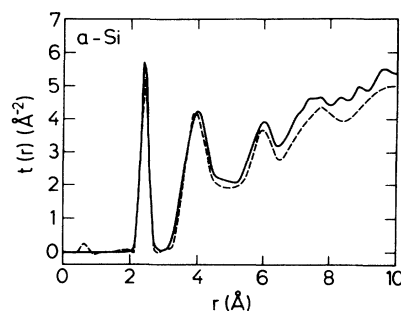


FIG. 1. Pair correlation function of the CDN model (solid line) compared to that derived from the neutron diffraction data (dashed line) of Ref. 1.

TABLE II. Ring statistics for the CDN model.

N=	5	6	7	8
Model	0.43	0.97	1.01	1.88
Diamond structure	0.00	2.00	0.00	3.00

is a member of a sevenfold ring and most are members of fivefold rings. No atom has a local ring structure that is indistinguishable from that of the diamond structure. By this measure of the local topology then, I can say that no atom lies in a local diamond-structure environment. Therefore I conclude that this model is a member of the purely amorphous class of structures.

What does this really mean? In one sense, it only means that every atom has an odd-membered ring passing through it. Quantitative measures of geometric distortion in amorphous silicon models are well developed. The rms bond-angle deviation has become almost a figure of merit for structural models. I believe it is equally, if not more, important to have a measure of the topological distortions in structural models. Here I propose the distribution of rings as one measure of the local topology. But it is probably not the best measure. Nevertheless, it provides an unequivocal distinction between structures with certain kinds of residual diamond-structure character and those without. Unfortunately, it is not a perfect distinction.

The structure factor of the model, which is related through a Fourier transform to the pair correlation function, is shown with  $Q$  along the [111] direction in Fig. 2. One would expect a small random intensity in the structure factor for a completely random collection of atoms. Any peaks in the structure factor would indicate some type of residual order in an amorphous structure. The CDN model has such residual order. This is apparent from the peaks at 2, 6, and 8  $\text{\AA}^{-1}$  that correspond to

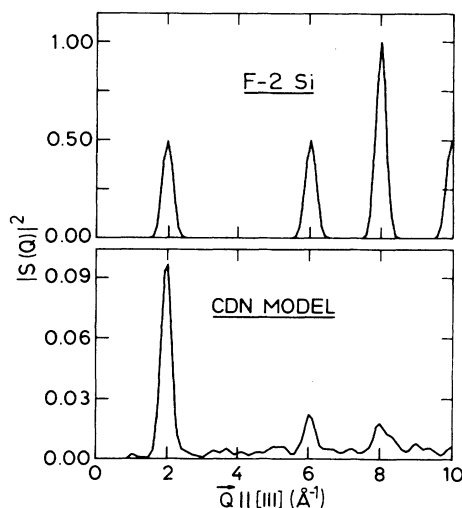


FIG. 2. Comparison of the structure factor of the CDN model with that of the diamond structure along the  $Q_{||[111]}$  direction.

those found in the structure factor of diamond-structure silicon. I believe that these peaks are due to the geometric constraints imposed by the maintenance of cubic boundaries in the model construction process. In particular, the use of  $8N^3$  atoms contained by cubic boundaries, just as in the diamond structure, seems always to lead to such residual peaks in the structure factor.<sup>14</sup> The structure factor for the model averaged over all directions shows good agreement with that of experiment, as might be expected from the agreement with the correlation function. The intermediate-range correlations necessary for the appearance of such peaks are not due to a memory of the diamond-structure topology because such an effect would be detected in the correlation function or the ring statistics.

Whether such residual intermediate-range correlations are also characteristics of real amorphous silicon is not clear from diffraction studies, but residual intermediate-range order has been inferred from electronic and optical studies on amorphous silicon.<sup>15</sup> In the case of laser-quenched amorphous silicon, which has been shown to exhibit a high degree of network order,<sup>16</sup> the amorphous material produced by the laser pulse ( $\sim 150$   $\text{\AA}$  thick) is surrounded by crystalline silicon. It is possible that the surrounding crystal imposes additional constraints on the topology of the amorphous layer similar to those imposed in the CDN model by the cubic boundaries. One could believe that a similar situation might also exist for amorphous silicon films deposited on single-crystal silicon substrates. The presence of residual intermediate-range order in a model might in fact be representative of some types of real amorphous silicon. However, it is not clear that such is the case for the correlations inferred in the present model.

The dihedral-angle distribution of the CDN model is compared with that of the diamond structure in Fig. 3. The statistical broadening about the two diamond-structure peaks also indicates the presence of residual order in the model. It is even less clear whether this should be viewed as a deficiency in the model structure. The dihedral-angle distortion is sensitive to the geometry and, to a lesser extent, the topology of the structure. As such, it should perhaps be expected that, like the bond lengths or bond angles, the dihedral angles will be distributed

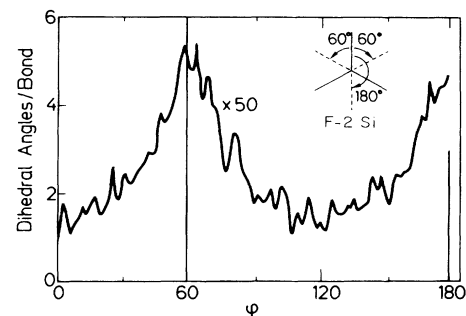


FIG. 3. Dihedral-angle distribution of the CDN model compared to that of the diamond structure. The latter consists of two delta functions at  $60^\circ$  and  $180^\circ$ .

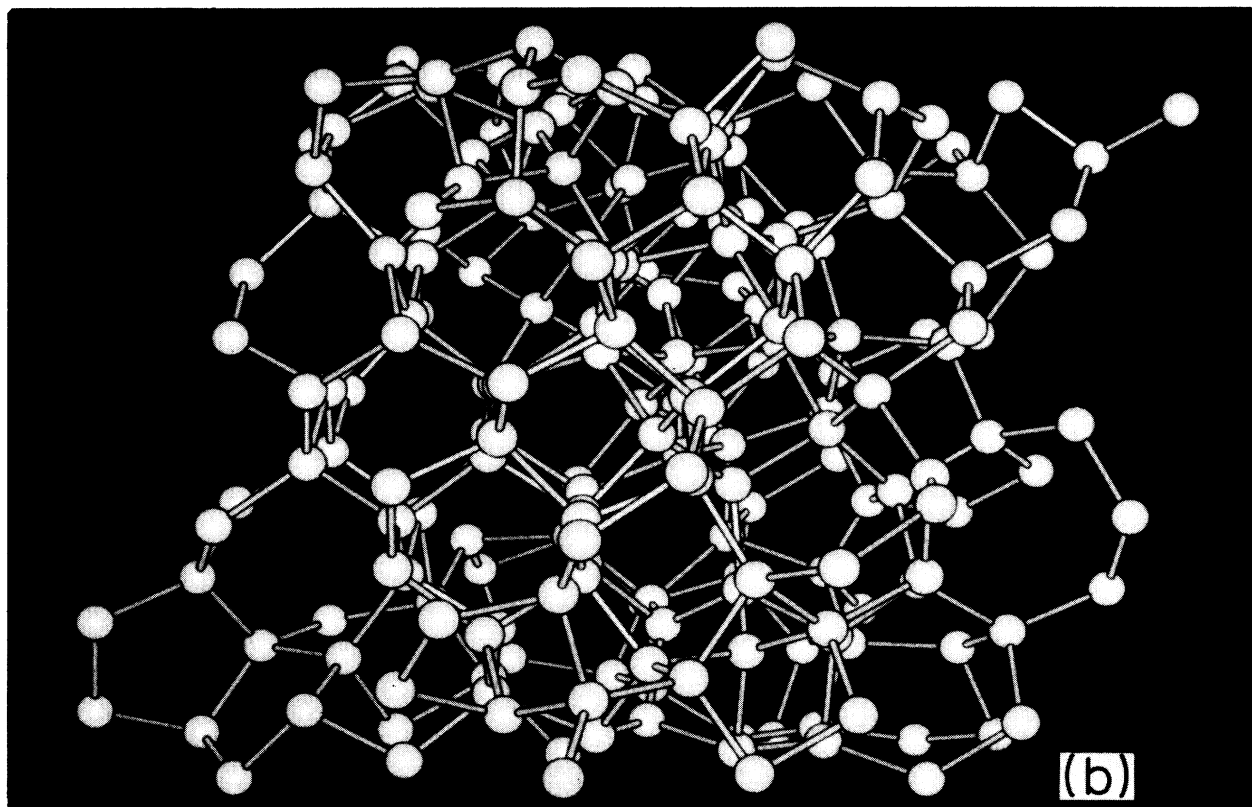
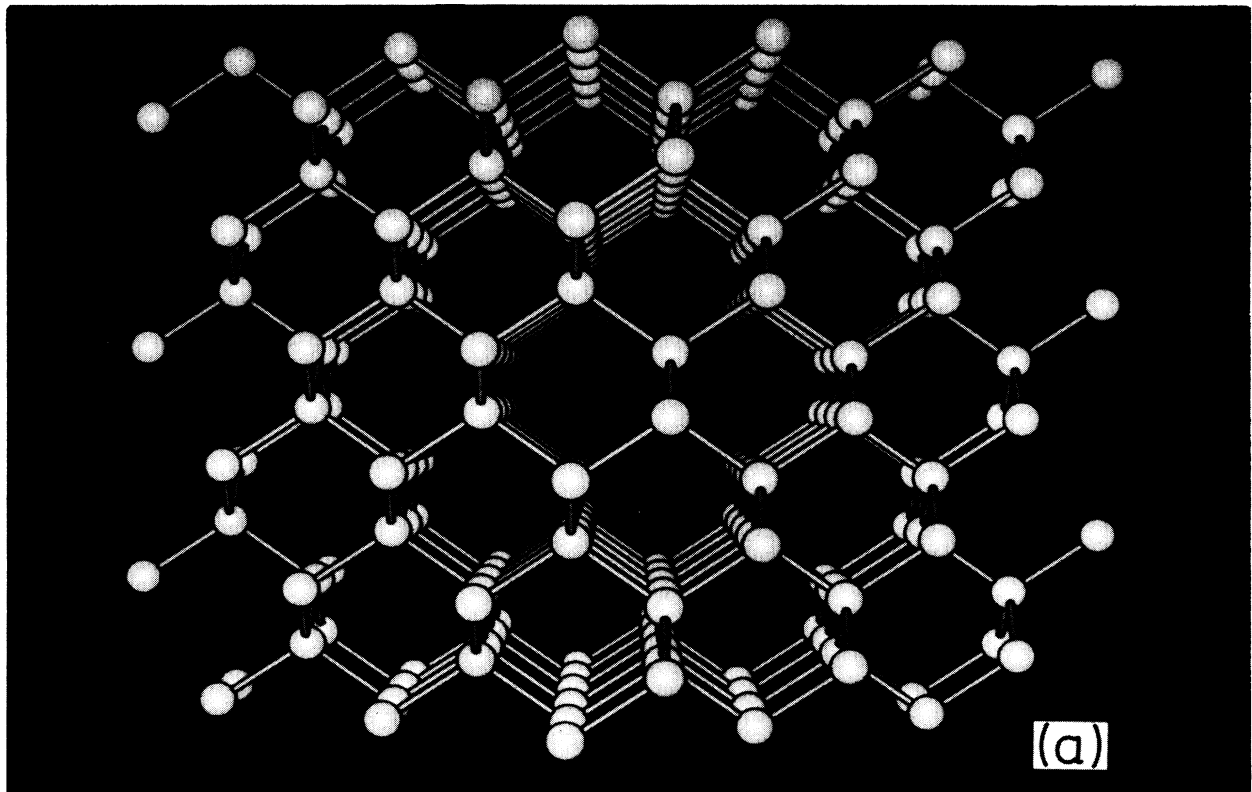


FIG. 4. Computer-generated pictures of (a) diamond-structure silicon and (b) the CDN model. View toward the (110) face.

about the diamond-structure values with the largest number of angles near  $60^\circ$  and  $180^\circ$ . It is interesting to note that the 2:1 ratio of  $60^\circ$  to  $180^\circ$  angles in the crystal is basically maintained in the area of the two main amorphous peaks.

Computer-generated pictures of the CDN model and diamond-structure silicon, with the view toward the (110) face, are shown in Fig. 4. Some remnants of the hexagonal cell structure remain in the amorphous network and the onset of diamond-structure ordering can be seen. In fact, only a few pairs of bond switches separate this structure from a partially crystalline configuration.<sup>17</sup> One can easily see the effect of bond breaking in the conversion of sixfold and eightfold rings into fivefold and sevenfold ones. In particular, one can see something of the distribution of rings passing through particular atoms on the (110) face. Such qualitative analysis is most easily performed by visual inspection.

The fact that only one or two pairs of bond switches are capable of removing an atom from oddfold ring membership does not necessarily mean that the structure as a whole occupies one of the lowest metastable states above the amorphous to crystalline transition. In the extreme case, one could have only one atom in a local diamond-structure environment and the rest of the structure could be grossly distorted. Yet it is the exhaustive nature of the WWW model construction algorithm that virtually guarantees that the local separation from the diamond structure will be small and roughly the same for each atom in the structure. On the basis of this homogeneity, the low geometric distortions, the reasonably good agreement with the experimental correlation function, and the lack of local diamond structure, I claim that the present CDN model is a close approximation to bulk, homogeneous amorphous silicon.

I cannot prove, however, that this model or similar models are necessarily representative of the bulk, homogeneous structure of real amorphous silicon films. I can show that the bulk properties of amorphous silicon can be well represented by applying simple, though realistic, interactions to the model structures. This is a necessary part of model evaluation in any case because many of the properties so far described are not subject to direct experimental confirmation. I chose the vibrational properties as the next step in model evaluation because of the simplicity of the calculations involved, the well-developed theory of lattice interactions for silicon structures, and the recent growth in experimental information concerning the vibrational properties of amorphous silicon through neutron scattering studies.

### III. VIBRATIONAL PROPERTIES OF THE CDN MODEL

Raman scattering and infrared transmission experiments continue to be the standard methods to obtain information regarding the phonons in amorphous silicon. These methods produce spectra that are related to the phonon density of states through the matrix elements, the exact nature of which is imprecisely known. Kamatikahara *et al.*<sup>18</sup> have recently performed neutron scattering

experiments on amorphous silicon thin films. Neutron scattering has the advantage of being independent of matrix element effects for high values of the momentum-transfer vector  $Q$ . The spectra derived from such experiments are expected to provide a more accurate measure of the phonon density of states of amorphous silicon.

The neutron scattering data is shown in Fig. 5 along with the phonon density of states for diamond-structure silicon<sup>9</sup> and the present CDN model. The  $k=0$  phonon density of states was calculated by diagonalizing the full dynamical matrix for the Keating potential or the full effective dynamical matrix (with bond charge degrees of freedom removed) for the Weber interactions. All vibrational spectra for the CDN model have been smoothed by applying Gaussian broadening (FWHM equals  $23 \text{ cm}^{-1}$ ) to the calculated histograms.

The phonon density of states for amorphous silicon derived from the neutron scattering experiments appears to be basically a broadened version of that for the crystal. There are four main features, corresponding to the TA-, LA-, LO-, and TO-phonon peaks in the crystal density of states. Kamatikahara *et al.* have noted three main differences between the phonon density of states of amorphous silicon derived from neutron scattering and that of diamond-structure silicon: (i) the peak at the top edge of the TA band observed in the crystal density of states is missing, (ii) the position of the LA feature occurs at lower frequency than in the crystal, and (iii) the relative intensity of the TO peak is smaller compared to that of the crystal.

The Weber interactions reproduce the phonon density of states of silicon in the diamond structure to within a few percent. It seems appropriate to look for an explanation of these differences in the phonon density of states of a reasonable structural model of amorphous silicon, such as the present CDN model, calculated with the Weber interactions.

The result of the calculation does not differ significantly from the result using the Keating potential (Fig. 6), although the phonon density of states derived from the Weber interactions is shifted uniformly to higher frequen-

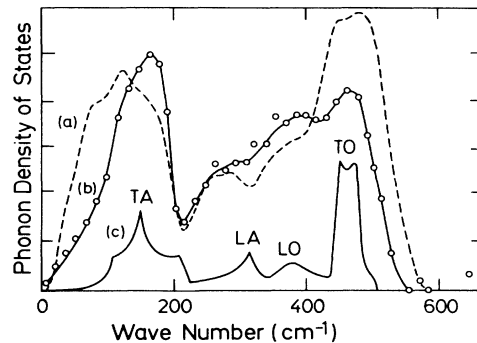


FIG. 5. Phonon density of states: (a) calculated for the CDN model; (b) obtained from neutron scattering measurements of amorphous silicon films (Ref. 18); and (c) calculated for silicon in the diamond structure by Weber (Ref. 9).

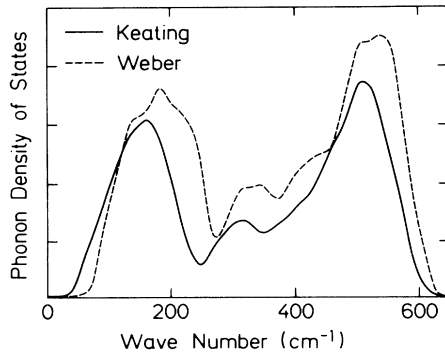


FIG. 6. Phonon density of states for the CDN model using Keating and Weber interactions.

cy due to the presence of deviations from the ideal crystal bond lengths.<sup>11</sup> Such a shift could be eliminated by scaling the parameters in the Weber model, as those in the Keating model have been scaled, to produce better agreement in terms of absolute peak positions. However, relative peak heights and positions are just as useful. Therefore I have shifted all vibrational spectra calculated for the CDN model with Weber's interactions by  $15 \text{ cm}^{-1}$  to lower energy to facilitate comparison with experiment.

I base the choice of the magnitude of the shift on the experimental observation that the amorphous TO-like band, while broader, is not significantly different from that of the crystal in terms of either shape or position. This follows directly from the preservation of short-range order in amorphous silicon and the dominant bond-stretching character of these modes. Aligning the TO-like peak of the calculated spectrum with that of the crystal requires only a small frequency shift and provides reasonable agreement with the experimental neutron scattering data. This gives me some confidence that the trends observed in the calculation, particularly the relative shift of peak positions, are real and not just an artifact of the choice of axes.

Because the calculated phonon densities of states derived from Weber's interactions and the Keating potential are fairly similar, I conclude that (1) the inclusion of long-range forces in the calculation of the vibrational properties of amorphous silicon has little effect and therefore is probably not necessary to understand the details of the vibrational spectra, and (2) these details depend mostly on the structure of the model used in the calculation.

The Weaire-Alben theorem<sup>19</sup> requires a dominant low- and high-frequency peak in the amorphous silicon phonon density of states purely as a result of the fourfold coordination and approximate tetrahedral bonding preserved in this phase. All structural models cannot help but reproduce these two peaks using a reasonable set of interactions. The two mid-frequency peaks, present in all experimental spectra, are usually missing from the phonon density of states calculated for poor structural models.<sup>20</sup> I believe that a calculated phonon density of states with the correct number of peaks and proper relative peak positions and intensities, as determined from experiment, is indicative of a realistic structural model.

The Weber-derived phonon density of states of the

CDN model (Fig. 5) also resembles very closely a broadened version of the density of states for silicon in the diamond structure, especially the TA- and TO-like peaks. The TA band appears to be substantially shifted to lower frequency, which may account for the missing high-frequency shoulder in the experimental spectrum. The TA modes also seem to be appreciably flattened, probably by the same mechanism that gives rise to their flattening in the crystal.<sup>9</sup> The resemblance of the TA-like peak of the amorphous silicon model to that of the crystal may be due in part to some residual diamond-structure ordering, but is more probably a natural result of employing Weber's interactions in the calculations. I note that the phonon density of states for germanium in the T-12 ("ST12") structure calculated with Weber's interactions also exhibits a marked flattening of the TA band.<sup>11</sup>

The calculation also shows a decrease in the frequency of the LA peak compared to the crystal density of states in agreement with the neutron diffraction data. However, I have no explanation for this behavior.

The large relative intensities of the LA and LO peaks and the reduced intensity of the TO peak found in the neutron scattering data are not well reproduced in the calculations for the CDN model. This is perhaps not surprising. The relative peak heights from the data are also at odds with those in the phonon density of states calculated for other *a*-Si models,<sup>21</sup> the diamond structure,<sup>9</sup> and the polymorphs B-8 ("BC8") Si and T-12 Ge.<sup>11</sup> There is some indication that the integrated intensity of the mid-frequency peaks increases with increasing topological distortion.<sup>11</sup> The low relative intensity of the TO-like peak is, however, less easily understood, but may be due to the presence of dangling bonds present in real amorphous silicon films.

One possible explanation for the large differences in the relative peak intensities observed in neutron scattering data for amorphous silicon compared with the results of calculations might be the use of neutron wave vectors ( $Q$ ) of insufficient magnitude. Weaire and Alben<sup>22</sup> have shown that the relative heights of the TA and TO peaks can vary significantly as a function of  $Q$ . Kamatikahara *et al.* claim to have averaged over sufficiently high- $Q$  values to reduce such variations to only a few percent. They propose that the lack of agreement between model calculations and experiment might be due to an underestimation in structural models of the bond-angle distortions present in real amorphous silicon films. However, the difficulty of achieving angular distortions in realistic structural models as low as those present in real films<sup>2</sup> argues against this view.

The dynamical structure factor calculated for the CDN model is compared to that derived from neutron scattering experiments on amorphous silicon<sup>23</sup> in Fig. 7. A range of phonon frequencies ( $86 \pm 6 \text{ cm}^{-1}$ ) was used in the calculation to offset the small sampling size and to approximate the resolution of the experimental data. The agreement between theory and experiment is reasonably good except that again the relative peak intensities are not well represented by the calculation.

The problem of interpreting the peak intensities in the phonon density of states derived from the neutron scatter-

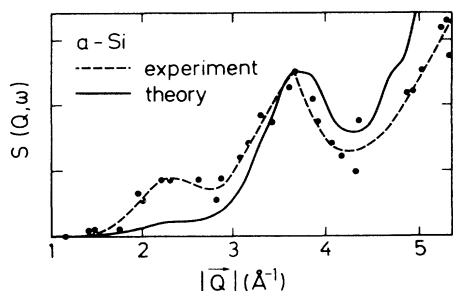


FIG. 7. Dynamical structure factor for *a*-Si. Dashed line taken from neutron scattering data ( $1/\lambda = 83 \text{ cm}^{-1}$ ) of Ref. 23. Solid line calculated from the phonon density of states of the CDN model using Weber's interactions.

ing experiments makes it desirable to use the Raman and infrared response of amorphous silicon as a further measure of the structure of the CDN model. This can only lead to indirect comparisons because I must rely on some approximations to describe the matrix element effects accompanying these two methods. Despite this drawback, comparisons between the calculated and experimentally measured quantities can be very useful.

I describe the infrared and Raman response of the CDN model in terms of a weighted density of states, whose weighting is determined from phenomenological expressions for the dipole moment and Raman tensor, respectively. These expressions result from a consideration of simple, intuitive models of the corresponding mechanisms involved. Most of these expressions have already been successfully applied to the study of distorted silicon structures.<sup>21</sup> Because the expressions explicitly depend on the eigenvectors and atomic coordinates, the details of the spectra very much depend upon the structural model underlying the calculations. I first examine the Raman response.

I use the formulation of Alben *et al.*<sup>21</sup> to describe the Raman response in amorphous silicon. The response is described in terms of three independent Raman tensors given by

$$\vec{\alpha}_1 = \sum_{l,i} (\hat{r}_{li} \hat{r}_{li} - \frac{1}{3} \vec{I}) \mathbf{u}_l \cdot \hat{r}_{li}, \quad (1)$$

$$\vec{\alpha}_2 = \sum_{l,i} (\hat{r}_{li} \mathbf{u}_l + \mathbf{u}_l \hat{r}_{li} - \frac{1}{3} \vec{I} \mathbf{u}_l \cdot \hat{r}_{li}), \quad (2)$$

$$\vec{\alpha}_3 = \sum_{l,i} \vec{I} \mathbf{u}_l \cdot \hat{r}_{li}, \quad (3)$$

where  $\mathbf{u}_l$  is the displacement of atom  $l$  for a particular mode,  $\vec{I}$  is the unit diadic, and  $\hat{r}_{li}$  is the unit vector from atom  $l$  to atom  $i$ .

The tensor  $\vec{\alpha}_1$  corresponds to changes in the polarizability due to pure stretching motions and has a characteristic depolarization ratio ( $\alpha_{xy}/\alpha_{xx}$ ) of  $\frac{3}{4}$  when averaged over a large, random (isotropic) sample. This mechanism gives rise to the sole Raman peak in diamond-structure silicon at  $520 \text{ cm}^{-1}$  with a strength of  $|4\sqrt{3}/9|^2$  per atom and an infinite depolarization ratio.  $\vec{\alpha}_2$  corresponds to

changes in the polarizability due to mixed stretching and bending motions and also has a characteristic  $\frac{3}{4}$  isotropic depolarization ratio.  $\vec{\alpha}_3$  depends only on bond compressions and has a depolarization ratio of zero. Of these three mechanisms, one would expect the first to be dominant in amorphous silicon as long as the departure from tetrahedral symmetry is not too severe. This is in fact the case for the CDN model as shown in Fig. 8. The contribution to the unpolarized Raman response ( $\alpha_{xx}^2 + \alpha_{xy}^2 + \alpha_{yx}^2 + \alpha_{yy}^2$ ) is shown for each mechanism separately. The calculations are compared to the reduced Raman spectrum from experiment.<sup>24</sup>

The sharp peak near  $520 \text{ cm}^{-1}$  in the Raman spectrum calculated for the CDN model due to the dominant  $\vec{\alpha}_1$  mechanism clearly results from the TO-like stretching similar to that observed for the diamond structure. The other two mechanisms are much weaker. It is surprising to see that  $\vec{\alpha}_2$  is weaker than  $\vec{\alpha}_3$  by a factor of 4. Alben *et al.*<sup>24</sup> ignored  $\vec{\alpha}_3$  in their treatment of the Raman response of amorphous silicon structural models because the experimental depolarization ratio of that time, 0.8, seemed to argue against its inclusion. The currently accepted value for the depolarization ratio for the TO-like peak of 0.53 (Ref. 25) and the larger contribution of  $\vec{\alpha}_3$  compared to  $\vec{\alpha}_2$  suggest that  $\vec{\alpha}_3$  cannot be properly ignored. However, because of the uncertainty in assigning coupling constants or treating interference terms, I have not tried to combine the mechanisms to fit the experimental data.

Alben *et al.*<sup>21</sup> have defined the infrared response in amorphous silicon in terms of phonon-induced charge fluctuations produced by bond-length distortions in adjacent pairs of bonds. The dipole moment is given by

$$\mu_1 = \sum_{l(i,j)} (\hat{r}_{li} - \hat{r}_{lj}) (\mathbf{u}_l \cdot \hat{r}_{li} - \mathbf{u}_l \cdot \hat{r}_{lj}). \quad (4)$$

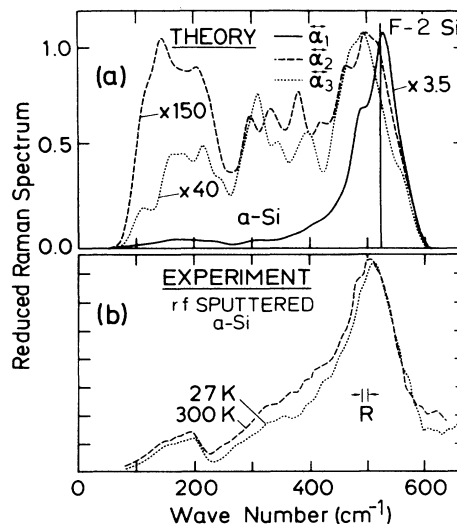


FIG. 8. Raman spectra of amorphous silicon: (a) the Raman response for the three mechanisms described in the text applied to the CDN model using Weber's interactions; (b) experimental Raman spectra measured from amorphous silicon films (Ref. 24).

The dipole moments arise from the transfer of negative charge from compressed to extended bonds. The infrared response for the CDN model due to this term is shown in Fig. 9(a). The spectrum is dominated by a central peak at  $300 \text{ cm}^{-1}$  with smaller wings at higher and lower frequency. A simple explanation for the enhancement of the mid-frequency modes for this mechanism has been given by Alben *et al.*<sup>21</sup>

The experimental infrared response of amorphous silicon is shown in Fig. 9(b). There are also four peaks as found in the neutron and Raman scattering experiments although the relative intensities are very different. The  $\mu_1$  mechanism does not adequately account for all four peaks. In particular the TA peak ( $\sim 150 \text{ cm}^{-1}$ ) is completely missing from the calculation. Shen *et al.*<sup>26</sup> have suggested that bond-angle distortions need to be taken into account to properly describe the infrared response in amorphous silicon. Because bond-angle distortions in amorphous silicon are always much larger than bond-length distortions, there is good reason to expect that the former might be important in any infrared response theory.

I therefore consider a second mechanism,<sup>27</sup> corresponding to phonon-induced charge fluctuations produced by distortions of the angle between adjacent pairs of bonds. The dipole moment is given by

$$\mu_2 = \sum_{l(i,j)} (\hat{r}_{li} + \hat{r}_{lj})(\mathbf{u}_{li} \cdot \hat{r}_{lj} + \mathbf{u}_{lj} \cdot \hat{r}_{li}). \quad (5)$$

Note that  $\mu_2$  is orthogonal to  $\mu_1$  for each bond pair. Both mechanisms give zero infrared activity when applied to the diamond structure as they should.

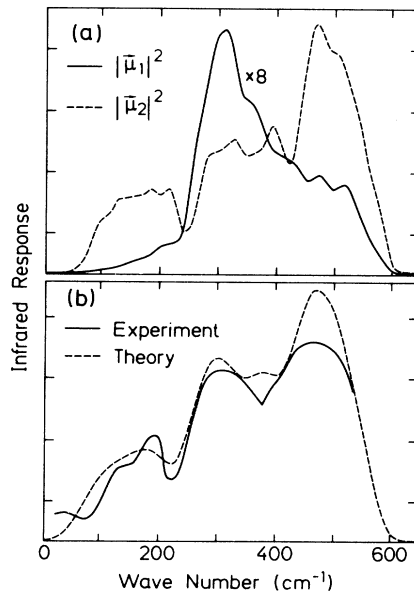


Fig. 9. Infrared spectra of amorphous silicon: (a) the infrared response for the two mechanisms described in the text applied to the CDN model using Weber's interactions; (b) a combination of the two mechanisms compared with the infrared absorption spectrum measured from amorphous silicon films (Ref. 26).

The contribution of  $\mu_2$  to the infrared response is also shown in Fig. 9(a). It clearly describes the experimental spectrum much better than  $\mu_1$ . It correctly exhibits four peaks of approximately the correct relative intensities and positions indicating that local charge transfer in amorphous silicon is mainly due to bond-angle distortions. These two mechanisms together provide a simple yet fairly complete description of the infrared activity in amorphous silicon. I have combined  $\mu_1^2$  and  $\mu_2^2$  in ratio 3:1 and compare the results to the experimental infrared spectrum in Fig. 9(b). The fit is good but there is no intrinsic significance to this ratio.

In general, using simple descriptions for the effects of matrix elements on the calculated phonon density of states I have been able to achieve reasonably good agreement with the experimental Raman and infrared data. The agreement between calculation and experiment is not independent of the model structure nor the corresponding phonon density of states. Indeed, without a good representation of the density of states that a realistic structural model implies, such good agreement with experiment could not be achieved.

In summary, I have shown that the CDN model has bond-length and bond-angle distortions near to those of real amorphous silicon and that its correlation function is in substantial agreement with experiment. The model has no local diamond-structure-like environments and is otherwise consistent with what one would expect for a purely amorphous structural model.

The vibrational density of states of the CDN model agrees well with the experimental neutron scattering data except for the relative intensities of the phonon peaks. The difficulties in explaining this aspect of the experimental neutron diffraction data for amorphous silicon make clear the desirability of systematic measurements of well-characterized samples with neutron, Raman, and infrared spectroscopies. Modifications of the phonon density of states of the model using simple, intuitive expressions for the Raman and infrared activities provide good agreement with the corresponding experimentally measured Raman and infrared spectra.

In general, the CDN model seems to be a fairly realistic representation of the bulk, homogeneous structure of amorphous silicon. Future studies of the effects of defects, impurities, or alloying on the vibrational or electronic properties of amorphous silicon can be carried out using this model with some confidence that its underlying bulk structure is basically correct.

#### ACKNOWLEDGMENTS

I thank D. Weaire and M. Cardona for useful comments and suggestions, and R. Strout for help with the data transfer. I would like to acknowledge the support of the Alexander von Humboldt-Stiftung. This work was partially performed under the auspices of the U.S. Department of Energy by Lawrence Livermore National Laboratory under Contract No. W-7405-Eng-48.



- <sup>1</sup>See for example, G. Etherington, A. C. Wright, J. T. Wenzel, J. C. Dore, J. H. Clark, and R. N. Sinclair, *J. Non-Cryst. Solids* **48**, 265 (1982).
- <sup>2</sup>F. Wooten and D. Weaire, *J. Non-Cryst. Solids*, **64**, 325 (1984).
- <sup>3</sup>D. E. Polk, *J. Non-Cryst. Solids* **5**, 365 (1971).
- <sup>4</sup>D. Henderson and F. Herman, *J. Non-Cryst. Solids* **8&10**, 359 (1972).
- <sup>5</sup>N. J. Shevchik, *Phys. Status Solidi B* **58**, 111 (1973).
- <sup>6</sup>L. Guttman, in *Tetrahedrally Bonded Amorphous Semiconductors—1974 (Yorktown Heights, New York)*, Proceedings of the Conference on Tetrahedrally Bonded Amorphous Semiconductors, AIP Conference Proc. No. 20, edited by M. H. Brodsky, S. Kirkpatrick, and D. Weaire (AIP, New York, 1974), p. 224.
- <sup>7</sup>F. Wooten, K. Winer, and D. Weaire, *Phys. Rev. Lett.* **54**, 1392 (1985).
- <sup>8</sup>P. N. Keating, *Phys. Rev.* **145**, 637 (1966).
- <sup>9</sup>W. Weber, *Phys. Rev. B* **15**, 4789 (1977).
- <sup>10</sup>K. Winer and F. Wooten, *Comput. Phys. Commun.* **34**, 67 (1984).
- <sup>11</sup>K. Winer and F. Wooten, *Phys. Status Solidi B* **136**, 519 (1986).
- <sup>12</sup>J. R. Blanco, P. J. McMarr, J. E. Yehoda, K. Vedam, and R. Messier, *J. Vac. Sci. Technol. A* **4**, 577 (1986).
- <sup>13</sup>R. H. Temkin, W. Paul, and G. A. N. Connell, *Adv. Phys.* **22**, 581 (1973).
- <sup>14</sup>F. Wooten, G. A. Fuller, K. Winer, and D. Weaire, Proceedings of the Seventh Winter Meeting on Low Temperature Physics, Mexico, 1986 (unpublished).
- <sup>15</sup>D. P. DiVincenzo, R. Mosseri, M. H. Brodsky, and J. F. Sadow, *Phys. Rev. B* **29**, 5934 (1984).
- <sup>16</sup>N. Maley, J. S. Lannin, and H. G. Cullis, *Phys. Rev. Lett.* **53**, 1571 (1984).
- <sup>17</sup>F. Wooten, G. Fuller, K. Winer, and D. Weaire, *J. Non-Cryst. Solids* **75**, 45 (1985).
- <sup>18</sup>W. A. Kamitakahara, H. R. Shanks, J. F. McClelland, U. Buchenau, F. Gompf, and L. Pintchovious, *Phys. Rev. Lett.* **52**, 644 (1984).
- <sup>19</sup>D. Weaire and R. Alben, *Phys. Rev. Lett.* **29**, 1505 (1972).
- <sup>20</sup>See for example, M. Ross, C. Perlov, C. Y. Fong, and L. Guttman, *J. Non-Cryst. Solids* **59&60**, 209 (1983); or D. Beeman, R. Tsu, and M. F. Thorpe, *Phys. Rev. B* **32**, 874 (1985).
- <sup>21</sup>R. Alben, D. Weaire, J. E. Smith, Jr., and M. H. Brodsky, *Phys. Rev. B* **11**, 2271 (1975).
- <sup>22</sup>D. Weaire and R. Alben, *J. Phys. C* **7**, L189 (1974).
- <sup>23</sup>W. A. Kamitakahara, H. R. Shanks, F. Gompf, and U. Buchenau, *Bull. Am. Phys. Soc.* **31**, 545 (1986).
- <sup>24</sup>J. E. Smith, Jr., M. H. Brodsky, B. L. Crowder, M. I. Nathan, and A. Pinczuk, *Phys. Rev. Lett.* **26**, 642 (1971).
- <sup>25</sup>D. Bermejo and M. Cardona, *J. Non-Cryst. Solids* **32**, 405 (1979).
- <sup>26</sup>S. C. Shen, C. J. Fong, M. Cardona, and L. Genzel, *Phys. Rev. B* **22**, 2913 (1980).
- <sup>27</sup>K. Winer and M. Cardona, *Solid State Commun.* **60**, 207 (1986).

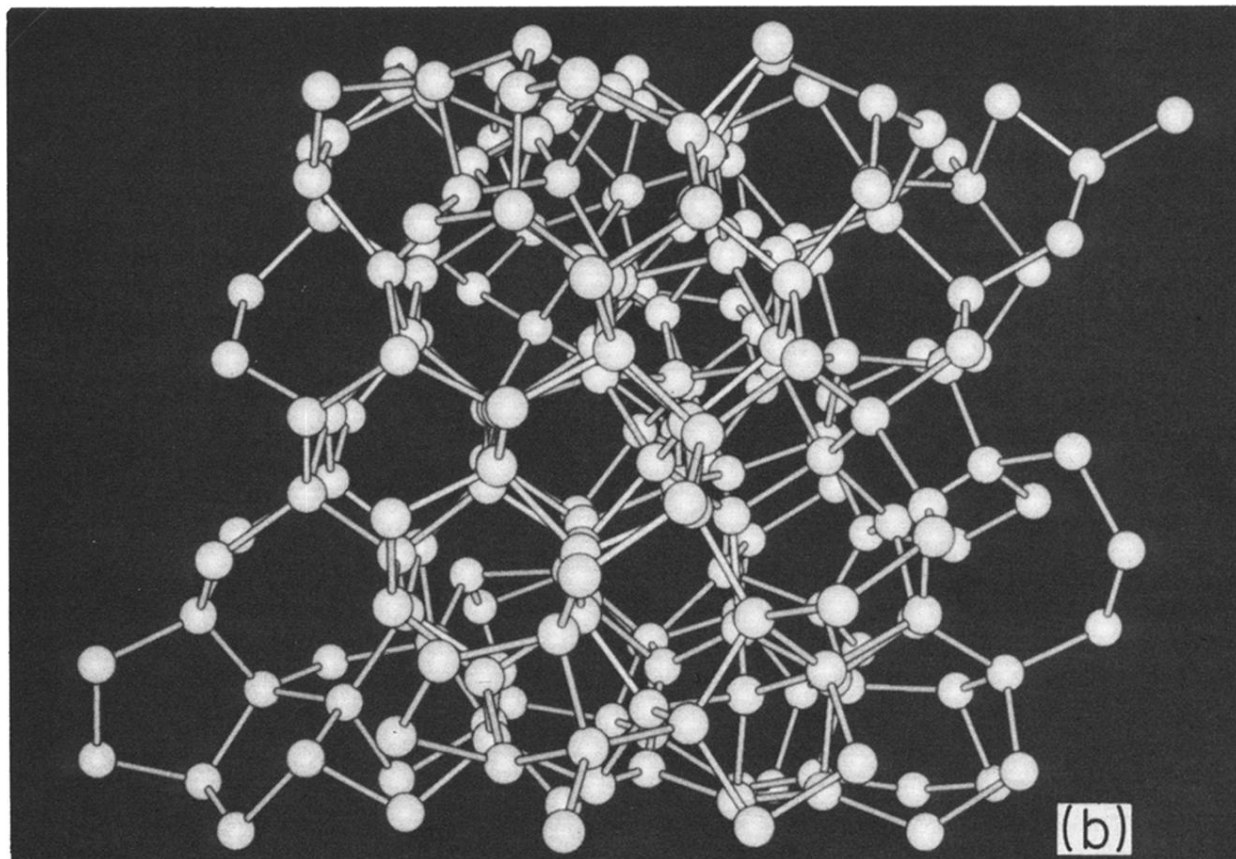
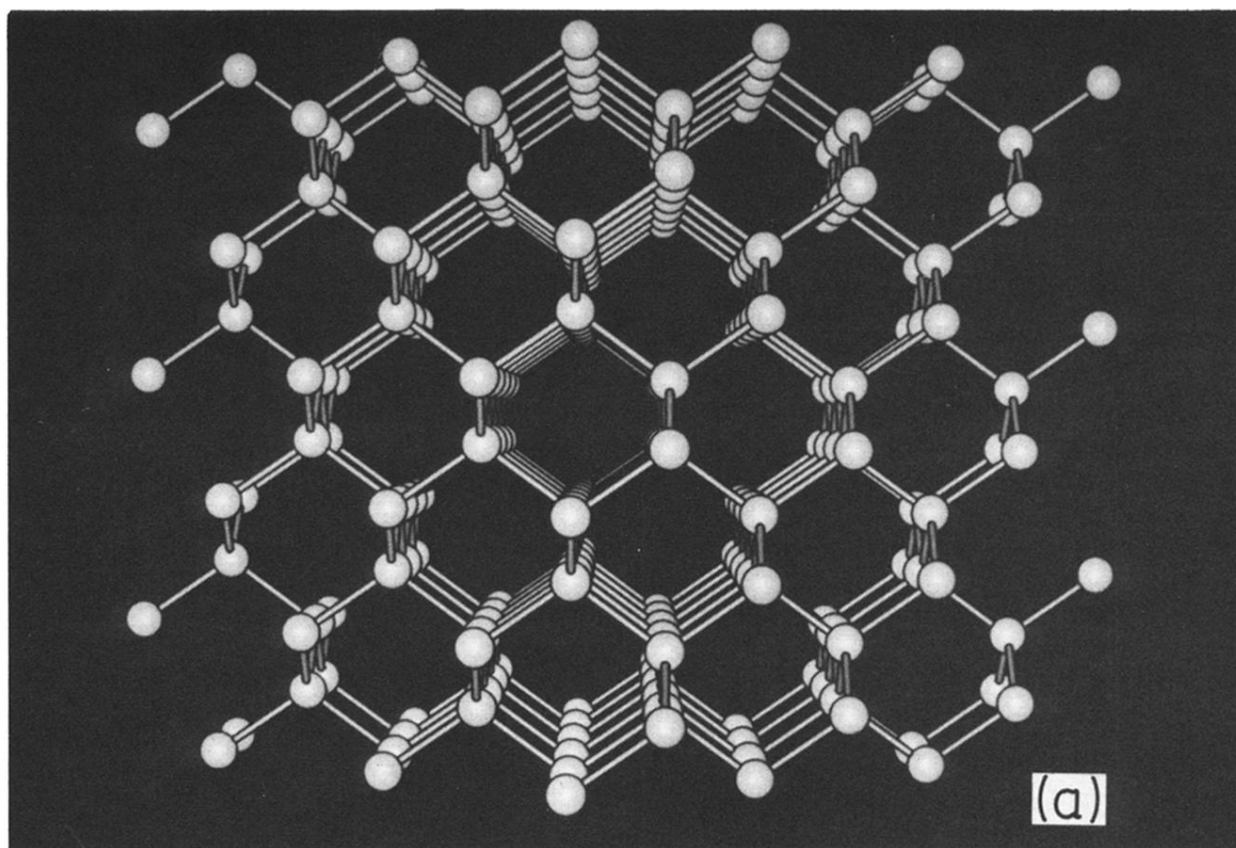


FIG. 4. Computer-generated pictures of (a) diamond-structure silicon and (b) the CDN model. View toward the (110) face.